ISSN: 0975-766X
CODEN: IJPTFI
Available Online through *Research Article*
www.ijptonline.com

AUTOMATED GLAUCOMA DIAGNOSIS FROM DIGITAL FUNDUS IMAGES USING ADVANCED CLASSIFIER ALGORITHM

Sai Prasanthi. B*[1], Logashanmugam E[2]
[1]Post Graduate Scholar, [2]Professor
[1,2]Department of Electronics and Communication Engineering, Sathyabama University, Chennai, India.
Email: iyer.prash93@gmail.com

Received on: 28-04-2017 *Accepted on: 05-06-2017*

Abstract

Automatic retinal image analysis is growing and is an important screening method for early detection of eye diseases. Glaucoma is a set of chronic eye conditions that damage the optic nerve due to increase in fluid pressure of the eye. It is a silent blinding disease also known as the 'Silent Thief' of the eye and individuals at the risk of developing glaucoma should be tested regularly to maintain their vision quality. There are many different tests that Ophthalmologists perform to monitor glaucoma, primarily, Ophthalmoscopy, Tonometry and Gonioscopy. These methods are very expensive, painful and may require experienced clinicians to do them. Therefore, there is a need to diagnose Glaucoma at a very beginning stage and accurately with low cost. In this paper, Steerable Pyramid Wavelet Transform was used for extracting the features. These extracted features were ranked based on the value feature selection algorithm. Then, these were used for the classification of normal and glaucoma images using Feed Forward Artificial Neural Network classifier.

Keywords: Glaucoma; Optic Nerve Head; Fundus images; Steerable Pyramid Wavelet; Correlation coefficient.

Introduction

Glaucoma is a group of eye conditions that result in the damage of eye vision [22]. It is often linked to a buildup of pressure within the eye, called the Intra Ocular Pressure (IOP), above the normal value estimated to be between 10mm Hg to 21mm Hg [1]. This increase in pressure can damage the nerves in the eye, which transmits images to the brain. If the damage continues, it would eventually lead to a permanent loss of vision. Thus, the detection at an early stage and treatment is the major key to prevent loss of vision [3]. Glaucoma is the third leading reason for visual impairment in India. Nearly 12 million people are affected by glaucoma every year. Glaucoma can affect any age group, including infants, children and elderly.

The wall of the eye ball is made up of three layers: Fibrous schlera and cornea; choroid, iris and the ciliary body and the retina. The Conjunctiva is a thin layer of tissue that sits on top of the eye. It protects the eye and also creates a surface underneath which loops the inside of the eyelid and form the backside of the eyeball. Cornea is on the same layer with the schlera, that is at the posterior end of the eyeball [21]. The iris has muscles, spinctem and dilator that contract and retract, which is responsible for the size of the pupil. It also makes the color of the eye. The pupil is the black part of the eye which captures the images. Behind the pupil are the lens that help in the change of shape. The primary structures are the lens and the cornea that bend the incoming light to focus the images on the retina at the back. The inner layer of the eyeball is the retina, which has the photoreceptors. The retina contains a section known as the fovea.

It has the cones of the eye, which are the photoreceptors. The retina captures the images through the photoreceptors. These images are sent to the nerve fibres that make the optic nerve also called the cranial nerve. The fluid within the eye is called the vitreous humor. It occupies the posterior of the eye. The posterior cavity is separated from the anterior cavity by the lens. The anterior cavity is further divided by the iris in to anterior chamber and the posterior chamber. The anterior cavity contains a fluid called the aqueous humor that carries the nutrients [21]. The aqueous humor is produced by the capillary network within the ciliary body and then it drains into the canal of sclemm before entering the blood.

The obstruction of this aqueous humor drainage leads to a group of eye disease called glaucoma. In a normal eye, the rate of secretion balances the rate of drainage. In a glaucoma eye, the drainage canal, canal of schlemm, is either partially or completely blocked. Fluid builds up in the chamber and this eventually increases the pressure within the eye. The pressure pushes the lens back and presses over the vitreous body which in turn compresses and affects the blood vessels and nerve fibers running behind the eye.

Types of Glaucoma

A. Open Angle Glaucoma

This is type of glaucoma accounts for at least 90% of all glaucoma cases. It is also known as the primary or chronic glaucoma. As the name suggests, the angle between the iris and the cornea is open [3]. Here, the drainage slowly gets clogged overtime.

Therefore, there is a gradual increase in the pressure on the optic nerve. This results in the decrease of peripheral vision. As the pressure increases, it eventually damages the central vision as well.

B. Closed Angle Glaucoma

Another main type of glaucoma is called the closed angle glaucoma where the angle is closed, causing an increase in the eye pressure. The rise in this pressure occurs suddenly or gradually. This gradual form of closure usually has no symptoms.

C. Normal Tension Glaucoma

This type is known as the low-tension glaucoma, which is characterized by progressive optic damage of t he nerve and loss of visual field with normal intraocular pressure. This is usually due to poor blood flow to the optic nerve that leads to the death of the nerve cells from retina to the brain.

D. Secondary Glaucoma

This type is due to the result of an eye injury, inflammation, and tumour and in advanced case of diabetes or by the use of drugs like steroids.

Manual Methodologies

A. Ocular Tonometry

A device called a Tonometer is used to measure the inner eye pressure [21]. The tonometers are calibrated to measure the pressure of the eye in millimetres of mercury. It touches the outside of the eye and records the pressure of the eye instantly.

B. Ophthalmoscopy

A special lens is used to detect the presence of glaucoma. This measures the colour and the shape of the optic nerve. A nerve that is cupped, not healthy or pink in colour is cause for concern. A confocal scanning method uses laser to produce a three-dimensional high resolution image of the nerves.

C. Perimetry

This method is a visual field test that produces a map of the vision field of the eye. But over 40% of the eye should be damaged before the visual field test diagnoses glaucoma.

D. Gonioscopy

In this method, a hand-held lens is placed on the eye. It helps in determining the angle between the iris and the cornea.

There are many more tests to diagnose glaucoma manually. But these tests are painful and difficult to perform and require trained clinicians to do them [21].

Literature Review

A. Automated Glaucoma Detection using OCT Images.

In [9], an algorithm for automated detection of glaucoma and classification by pixel grouping using super pixel classification was proposed. This method extracted features like RNFL thickness and reflectivity from the OCT (Optical Coherence Tomography) images and then they were combined to obtain a feature map. Then, the feature map was segmented in to hundred parts using the pixel segmentation. Feature vector was calculated using histogram distribution, mean and standard deviation of each super pixel.

B. Image preprocessing based on illumination correction.

In [17], illumination correction, Optic Head Normalization and vessel removal for the pre-processing of the fundus images were used. The illumination method correction method removes the retinal background from the original image to get an evenly illuminated fundus image. The estimation is done by average intensity filtering. The vessel structures in the eye ground were removed by using segmentation and also the convergence of vessel-tree were applied for ONH normalization.

C. Automated Glaucoma Detection using Histogram Features.

In [16], both magnitude and phase components of the histogram features are computed. First, the Region Of Interest (ROI) was selected, then Gabor Filtering was applied and then Local Binary Pattern (LPB) was performed to extract the features. Daugman's algorithm was used to accomplish feature set extraction. Image is then transformed into an array using image operators which forms the histogram features for image analysis. Euclidean distances are analyzed. The system produced a sensitivity of 95.45%. It uses a predefined value for all the images.

Automated Glaucoma Diagnosis

The R, G, B and the gray components are extracted from the normal and the glaucoma images. The R, G, B components and the gray scale components are subjected to Steerable Pyramid Wavelet Transform. The R, G and B components of the image consists of significant details in the form of variation in the gray pixel intensities. The sub-band images are then feature extracted based on their correntropy feature. The extracted features are then classified into normal and glaucoma images by using the Feed Forward Artificial Neural Network Classifier Algorithm.

A. Steerable Pyramid Wavelet Transform The Steerable Pyramid is a linear multi-scale, multi-orientation image decomposition which is useful for image-processing and machine vision applications. It was developed to overcome the drawbacks of orthogonal separable wavelet decompositions. Once the orthogonality constraint is dropped, it is

easier to implement a filter design [7]. The basis functions of the steerable pyramid are Kth-order directional derivative operators (for any choice of K), that come in different sizes and K+1 orientations. As a directional derivative, they have a rotation-invariant subspace, and designed and sampled so that the whole transform forms a tight frame. The block diagram for the decomposition is shown. First, the image is being separated into lowpass and highpass subbands, using the filters L_0 and H_0. The lowpass subband is further divided into a set of oriented bandpass subbands and a lower pass subband. This lower pass subband is then sub-sampled by a factor of 2 in the X and Y directions.

B. Feature extraction

Correlation coefficient is used for identifying the features from the acquired normal and glaucomatous images. A Correlation Coefficient is a number that measures a sort of connection and reliance, which is the factual connections between at least two qualities or features [23]. The relationship coefficient is a factual measure of how well the patterns in the anticipated qualities take after the patterns in the past genuine qualities.

The MATLAB syntax for correlation coefficient is given below,

$$R = corrcoef(A) \qquad (1)$$

It gives the correlation coefficient (R) of A. A is a matrix whose columns represent random variable and rows represent observations.

The mathematical formula for correlation coefficient is given as

$$r = \frac{N\sum xy - (\sum x)(\sum y)}{\sqrt{[N\sum x^2 - (\sum x^2)][N\sum y^2 - (\sum y^2)]}} \qquad (2)$$

where N is the number of pairs, $\sum xy$ is the sum of products of the pairs, $\sum x$ is the sum of x, $\sum y$ is the sum of y, $\sum x^2$ is the sum of squared x and $\sum y^2$ is the sum of squared y.

Feature Standardization

In this paper, features are standardized using the mean and the standard deviation method. This method is called the z-score normalization [8]. Here, the mean is subtracted from the data and is then divided by the standard deviation. If a is the mean and $\dot{a}$ is the standard deviation, then the normalized data is given as,

$$\hat{a} = \frac{a \dot{-} \dot{a}}{\dot{a}} \qquad (3)$$

ANN Classifier Algorithm

The features are classified using the ANN (Artificial Neural Network) classifier algorithm. The type of ANN classifier used is the Feed Forward with Back Propagation Artificial Neural Network classifier algorithm.

The Feed Forward ANN consists of layers of processing units with each layer feeding input to the next layer in a feed forwarding mechanism through a set of connection set weights [19]-[20]. The operation phase of a Feed Forward Network is classified in to: Learning phase and Classification phase. The Feed Forward uses a supervised learning algorithm for discriminating the classes. Each neuron in one layer is connected with all the neurons in the other layers [18]. The connection between the two neurons i and j is determined by the weight w_{ij} and the i^{th} neuron by ϑ_{ij}, the threshold coefficient. The output value of the neuron i is determined by,

$$x_i = f(\xi_i) \qquad (4)$$

$$\xi_i = \vartheta_i + \sum_{j \in r_i^{-1}} w_{ij} x_i \qquad (5)$$

where ξ_i and $f(\xi_i)$ are the potential and transfer function of the i^{th} neuron respectively. The transfer function is given by,

$$f(\xi_i) = \frac{1}{1+\exp(-\xi)} \qquad (6)$$

The minimisation of the objective (E) function is given by,

$$E = \sum_o \frac{1}{2} (x_o - \ddot{x}_o) (7)$$

where, x_o and $\ddot{x}_o$ are the vectors having the neuron's output values and summation over input neurons o [18].

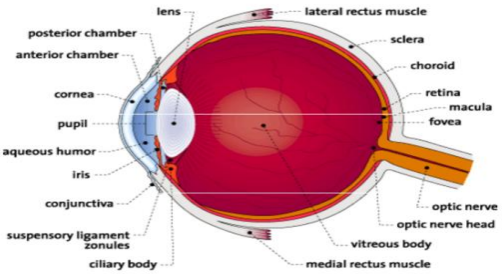

Fig.1 Ocular Anatomy.

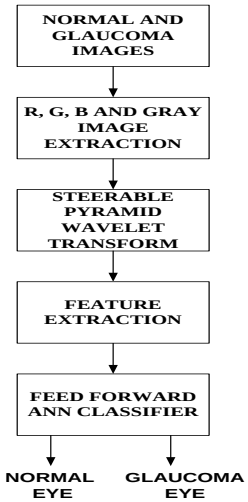

Fig. 2 Block diagram of the proposed method.

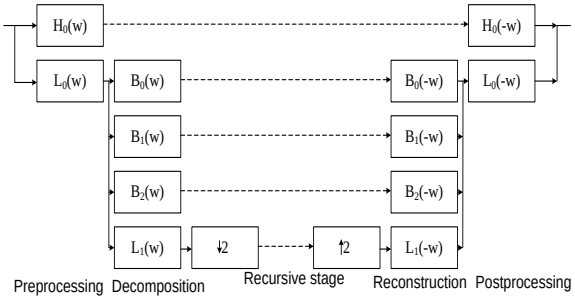

Fig. 3 Steerable pyramid filter.

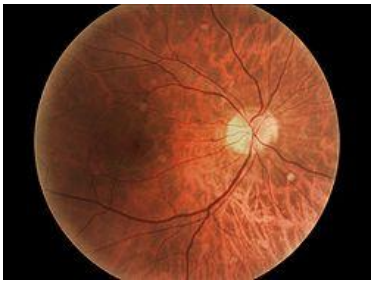

Fig. 4 Sample fundus image.

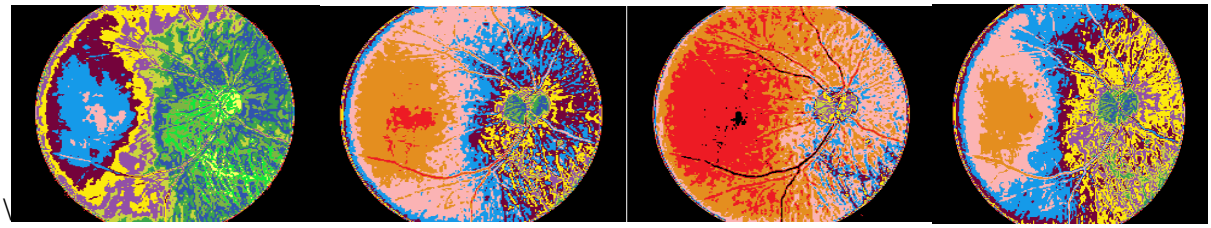

(a) (b) (c) (d)

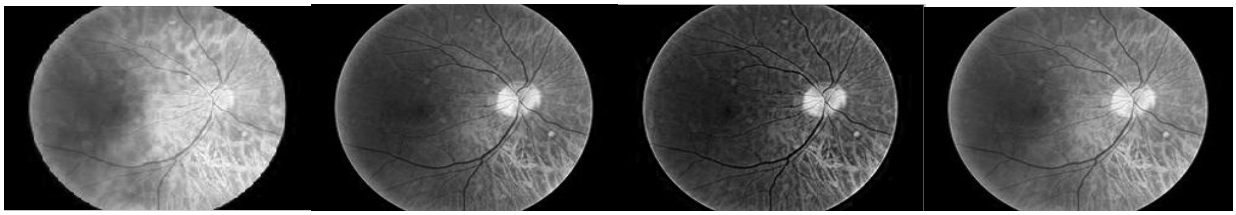

(e) (f) (g) (h)

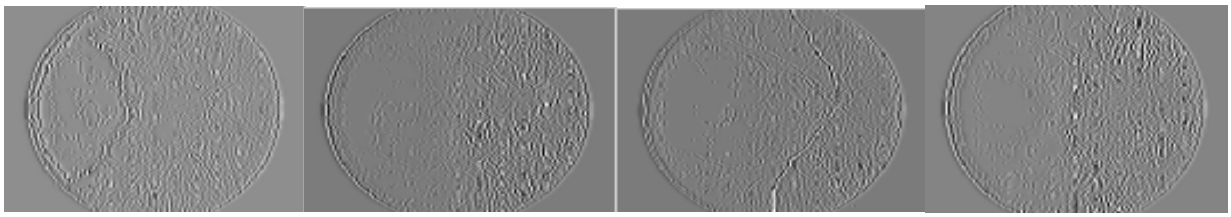

(i) (j) (k) (l)

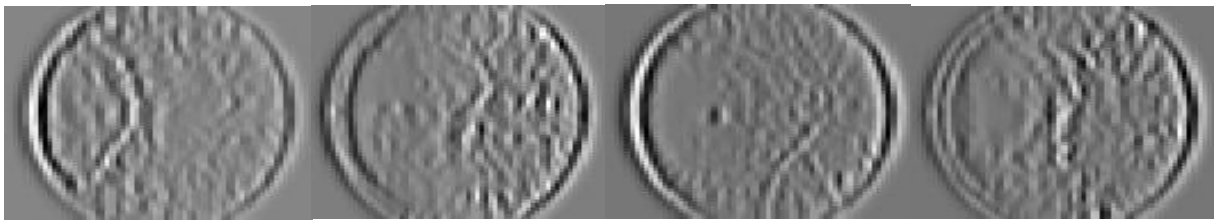

(m) (n) (o) (p)

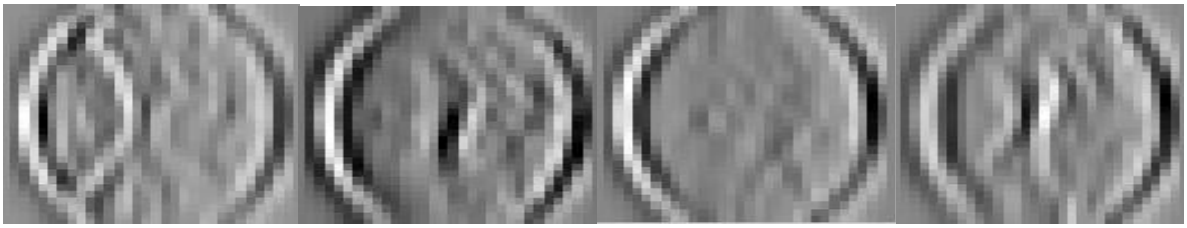

(q) (r) (s) (t)

Fig. 5: Fig. 5(a), 5(b), 5(c) and 5(d) are the pseudo color maps of red, green, blue and grayscale images of fig. (4). Fig. 5(e), (i), (m) and (q) are steerable pyramid wavelet components of Fig. 5(a). Fig. 5(f), (j), (n) and (r) are steerable pyramid wavelet components of Fig. 5(b). Fig. 5(g), (k), (o) and (s) are steerable pyramid wavelet components of Fig. 5(c). Fig. 5(h), (l), (t) and (t) are steerable pyramid wavelet components of Fig. 5(d).

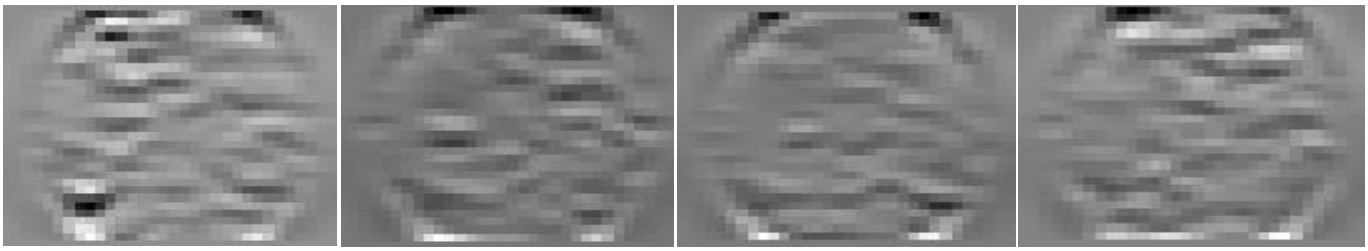

(a) (b) (c) (d)

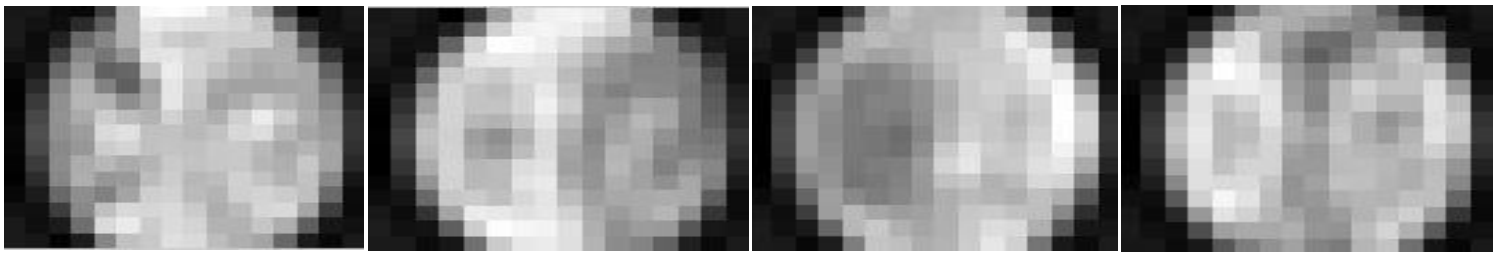

(e) (f) (g) (h)

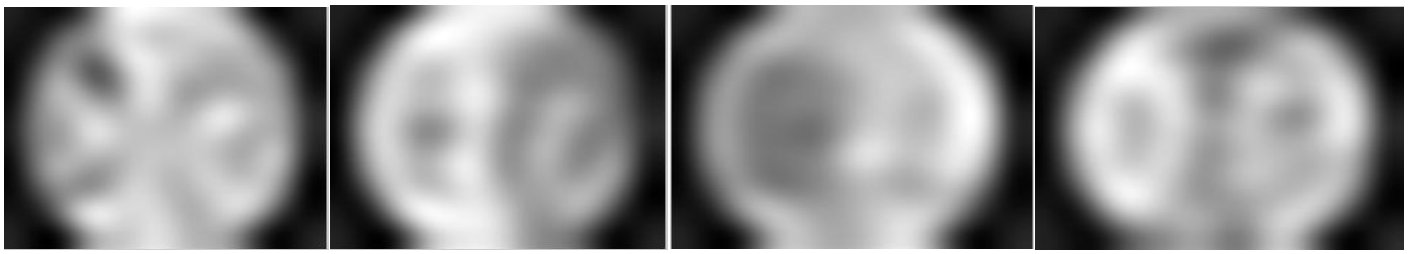

(i) (j) (k) (l)

Fig. 6: Fig. 6 (a) and (e) are steerable pyramid wavelet components of Fig. 5(a). Fig. 6 (b) and (f) are steerable pyramid wavelet components of Fig. 5(b). Fig. 6 (c) and (g) are steerable pyramid wavelet components of Fig. 5(c). Fig. 6 (d) and (h) are steerable pyramid wavelet components of Fig. 5(d). Fig. 6 (i), (j), (k) and (l) are the reconstructed images of the fig. 5 (a), (b), (c) and (d) respectively.

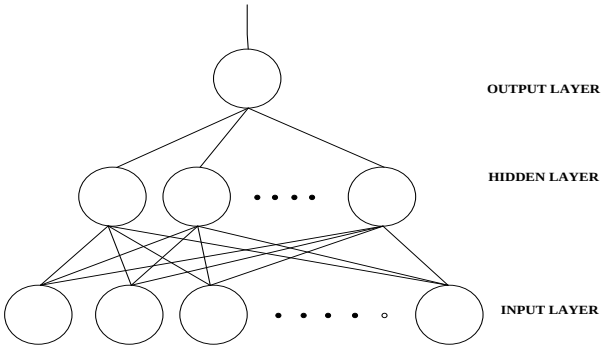

Fig.7 A typical multi-layered feed forward network.

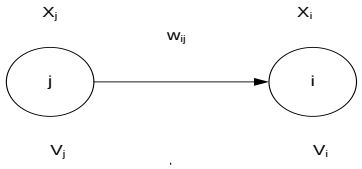

Fig. 8 Connection between two neurons.

Table I: Advantage of Steerable Wavelet Transform over the other transforms.

	Steerable Pyramid	Ortho Wavelet	Laplacian Pyramid	Gabor Transform	Block DCT
Jointly Localized	Yes	Yes	Yes	Not inverse	No
Tight frame	Yes	Yes	No	No	Yes
Oriented kernels	Yes	No	N/A	Yes	No
Translation invariant	Yes	No	Yes	No	No
Rotation invariant	Yes	No	N/A	No	No
Over-completeness	4k/3	1	4/3	1	1

Conclusion

In this paper, an automated glaucoma diagnosis system has been developed. The Steerable pyramid wavelet transform was used to extract the features from the digital fundus images. Correlation coefficient was used for finding out the relation between the extracted features. The mean and standard deviation algorithm was used for standardization of the features. Finally, the Feedforward Artificial Neural Network classifier algorithm was used to classify the images as normal or glaucomatous eye. The normal and glaucoma images for experimenting were collected from High Resolution Fundus (HRF) Image Database. The application of the proposed method can be further extended to diagnose diabetic retinopathy, colour blindness, cancer, etc.

References

1. Bock. R, J. Meier, L. G. Nyúl , J. Hornegger , G. Michelson. “Glaucoma risk index: Automated glaucoma detection from Colour fundus images,” Medical Image Analysis, vol. 14, no. 3, pp. 471–481, 2010.

2. Ghafar. R. “Detection and characterisation of the optic disc in glucoma and diabetic retionopathy,” in Medical Image Understand Annual Conference, (London, UK), pp. 23–24, September 2004.
3. Glaucoma Research Foundation- funding innovative research to find a cure for glaucoma. 251 post street, suite 600, San Francisco, CA.
4. Greaney. M.J., “Comparison of optic nerve imaging methods to distinguish normal eyes from those with glaucoma,” Investigative Ophthalmology and Visual Science, vol. 43, no. 1, pp. 140–145, 2002.
5. Itai N, Tanito M, Chihara E. Comparison of optic disk topography measured by Retinal Thickness Analyzer with m e a s u rement by Heidelberg Retina Tomograph II. Jpn J Ophthalmol 2003; 47: 214-20.
6. Kocak I, Zulauf M, Bergamin O. Evaluation of the Brusini glaucoma staging system for typing and staging of perimetric results. Ophthalmologica 1998.
7. Mookiah. M., “Data mining technique for automated diagnosis of glaucoma using higher order spectra and wavelet energy features,” Knowledge-Based Systems, vol. 33, pp. 73–82, 2012.
8. U. Rajendra Acharya, SumeetDua, Xian Du, “Automated diagnosis of glaucoma using texture and higher order spectra features”, IEEE Transactions on Information Technology In Biomedicine, May 2011, pp 449-455.
9. Xu, J., Ishikawa, H., Wollstein, G., & Schuman, J. S. (2011, August). “3D optical coherence tomography super pixel with machine classifier analysis for glaucoma detection”, Engineering in Medicine and Biology Society, EMBC, Annual International Conference of the IEEE, pp.3395-3398, IEEE, 2011.
10. Alghmdi, H. Hongying Lilian Tang, M. Hansen, A. O'Shea, L. Al Turk and T. Peto, “Measurement of optical cup-to-disc ratio in fundus images for glaucoma screening” International Workshop on Computational Intelligence for Multimedia Understanding (IWCIM), pp. 1-5, IEEE 2015.
11. A, Murthi, and M. Madheswaran, “Enhancement of optic cup to disc ratio detection in glaucoma diagnosis”, International Conference on Computer Communication and Informatics (ICCCI), pp.1-5, IEEE 2012.
12. E. A. Essock, “Analysis Of Gdx-VccPolarimetry Data By Wavelet-Fourier Analysis Across Glaucoma Stages”, Invest. Ophthalmol, Vol. 46 Issue 8, pp:2838-2847, 2005.
13. Hafsah Ahmad, AbubakarYamin, Aqsa Shakeel, Syed Omer Gillani and Umer Ansari “Detection of Glaucoma Using Retinal Fundus Images”, 2014 IEEE.
14. Joshi, G, Sivaswamy, Krishnadas, S.R. “Depth discontinuity-based cup segmentation from multi-view colour retinal images”, IEEE Transactions on Biomedical Engineering, Volume: 59, pp. 1523 – 1531, 2012.

15. U. R. Acharya, K. S. Vidya, D. N. Ghista, W. J. E. Lim, F. Molinari, and M. Sankaranarayanan, "Computer aided diagnosis of diabetic subjects by heart rate variability signals using discrete wavelet transform method," Knowledge-Based Systems, vol. 81, pp. 56 – 64, 2015.
16. Karthikeyan Sakthivel and RengarajanNarajanan, "An automated detection of glaucoma using histogram features".
17. M. Mishra, M. K. Nath and S. Dandapat, "Glaucoma detection from color fundus images", International Journal of Computer & Communication Technology, Vol. 2 Issue 6, 2011.
18. Daniel Svozil A, Vladimir KvasniEka B, JiEPospichal B, "Chemametric and intelligent laboratory systems", 1997.
19. Yegnanarayana E, "Aritificial Neural Networks", prentice hall of india private limited, 2003.
20. Lynne E Parker, "Notes on multilayer, feedforward neural networks", Machine Learning, 2007.
21. Vail Derreck, "American Journal of Ophthalmology", Volume 24, Issue 5, May 1941, Pages 587-588.
22. Srinivasan Aruchamy, ParthaBhattacharjee and GoutamSanyal, "Automated Glaucoma Screening in Retinal Fundus Images", International Journal of Multimedia and Ubiquitous Engineering, Vol.10, No.9, 2015.
23. D. Sasikala, R. Neelaveni, "Correlation coefficient measure of Multimodal brain image registration using fast Walsh hadamard transform" journal of theoretical and applied information technology, 2010.
24. K. Bharathi, S. Karthikeyan. " A novel implementation of image processing for extracting abnormal images in medical application", IJST, 2015.